Geomechanics and Engineering, *Vol. 25, No. 2 (2021) 123-134*
DOI: https://doi.org/10.12989/gae.2021.25.2.123

Quantitative assessment on the reinforcing behavior of the CFRP-PCM method on tunnel linings

Wei Han[1], Yujing Jiang*[1], Xuepeng Zhang[2], Dairiku Koga[3] and Yuan Gao[1]

[1]*Graduate School of Engineering, Nagasaki University, Nagasaki 852-8521, Japan*
[2]*College of Energy and Mining Engineering, Shandong University of Science and Technology, Qingdao 266590, China*
[3]*Department of Disaster Management, Engineering Consultants Co., Fukuoka 812-0013, Japan*

(Received July 1, 2020, Revised March 22, 2021, Accepted March 30, 2021)

Abstract. In this paper, the carbon fiber reinforced plastic (CFRP) grids embedded in polymer cement mortar (PCM) shotcrete (CFRP-PCM method) was conducted to repair the degraded tunnel linings with a cavity. Subsequently, the reinforcing effect of the CFRP-PCM method under different degrees of lining deterioration was quantitatively evaluated. Finally, the limit state design method of the M-N interaction curve was conducted to determine whether the structure reinforced by the CFRP-PCM method is in a safe state. The main results indicated that when the cavity is at the shoulder, the lining damage rate is more serious. In addition, the remarkably reinforcing effect on the degraded tunnel linings could be achieved by applying a higher grade of CFRP grids, whereas the optimization effect is no longer obvious when the grade of CFRP grids is too high (CR8); Furthermore, it is found that the M-N numerical values of the ten reinforcing designs of the CFRP-PCM method are distributed outside the corresponding M-N theoretical interaction curves, and these designs should be avoided in the corresponding reinforcing engineering.

Keywords: CFRP-PCM method; degraded tunnel lining; deterioration degree; M-N interaction curve

1. Introduction

In the last few decades, a great quantity of tunnels (water supply, metro, railway, road, etc.) have been constructed in the world (Aalianvari *et al*. 2017, Ghasemi and Nowak 2018, Schrefler *et al.* 2011). Among the tunnel supporting structures, the lining is the main guarantee for their long-term safe operation (Tonon 2010). However, as time passed, many of them show signs of deterioration with forms of cracking, spalling, and collapse, seriously threatening the safety of tunnel operation. Since the degraded lining concrete cannot be easily replaced, it is vital to search for suitable methods that can effectively reinforce the degraded tunnel linings.

Various techniques have been proposed to repair the concrete diseases and ensure the serviceability of the structure, such as the fiber-reinforced shotcrete method (Li *et al.* 2017, Guler *et al.* 2018, Joong *et al*. 2016, Guler *et al.* 2019, Jeng *et al*. 2002, Sukontasukkul *et al.* 2018, Guler *et al.* 2021, Guler and Yavuz 2019), the carbon fiber sheet method (Lee and Lee 2002), the steel board method (Kishi *et al*. 2005), and the fiber reinforced plastic (FRP) method (Gaurav and Signh 2018, Mofidi and Chaallal 2014). Generally, the FRP composites have emerged as one of the most existing and promising reinforced technologies due to its favorable properties, such as high strength-weight ratio, short installation period, and adaptability to curved surfaces (Singh and Patra 2020, Rajak *et al.* 2019). In recent years, a new type of FRP composite material, CFRP grid, has been proposed for structural repair (Nishi *et al.* 2012, Benzaama *et al.* 2018, Guo *et al.* 2018). Concerning the reinforcing effect of CFRP composites on the reinforced concrete (RC), Jeffrey *et al.* (2016) conducted the punching shear tests to access the shear capacity of concrete decks reinforced by FRP grids. Maalej and Leong (2005) experimental investigated the interfacial shear stress and the failure modes of RC beams strengthened in flexural with CFRP composites. Rabia *et al.* (2019) investigated the effect of the porosity on the shear interfacial stresses of the beam strengthened with FRP composites, and the reinforcing effect was also clarified. Fang *et al*. (2016) conducted a four-point bending experiment of composite concrete slabs reinforced by CFRP grids, and the effects of CFRP grid rib spacing, grid rib height and sheet thickness were considered. In addition, other investigations proposed that beams reinforced by CFRP can better avoid debonding failure, resulting in good strength and ductility (Sumathi and Arun 2017, Razavi and Mustaffa 2018, Makeev *et al.* 2019).

Some materials have been recently regarded as the protection substance, for example, polymer cement mortar (PCM) (Feiteira and Ribeiro 2013, Bansal and Sidhu 2017, Guo *et al.* 2018). According to the FRP Grid Method Association of Japan, the construction processes of the CFRP-PCM method on degraded tunnel linings can be presented in Fig. 1. At first, vacuum blasting the surface of the existing degraded lining concrete. Then, repair the lining surface to make it as flat as possible to ensure better reinforcement for the CFRP-PCM method. Subsequently,

*Corresponding author, Professor
E-mail: jiang@nagasaki-u.ac.jp

ISSN: 2005-307X (Print), 2092-6219 (Online)

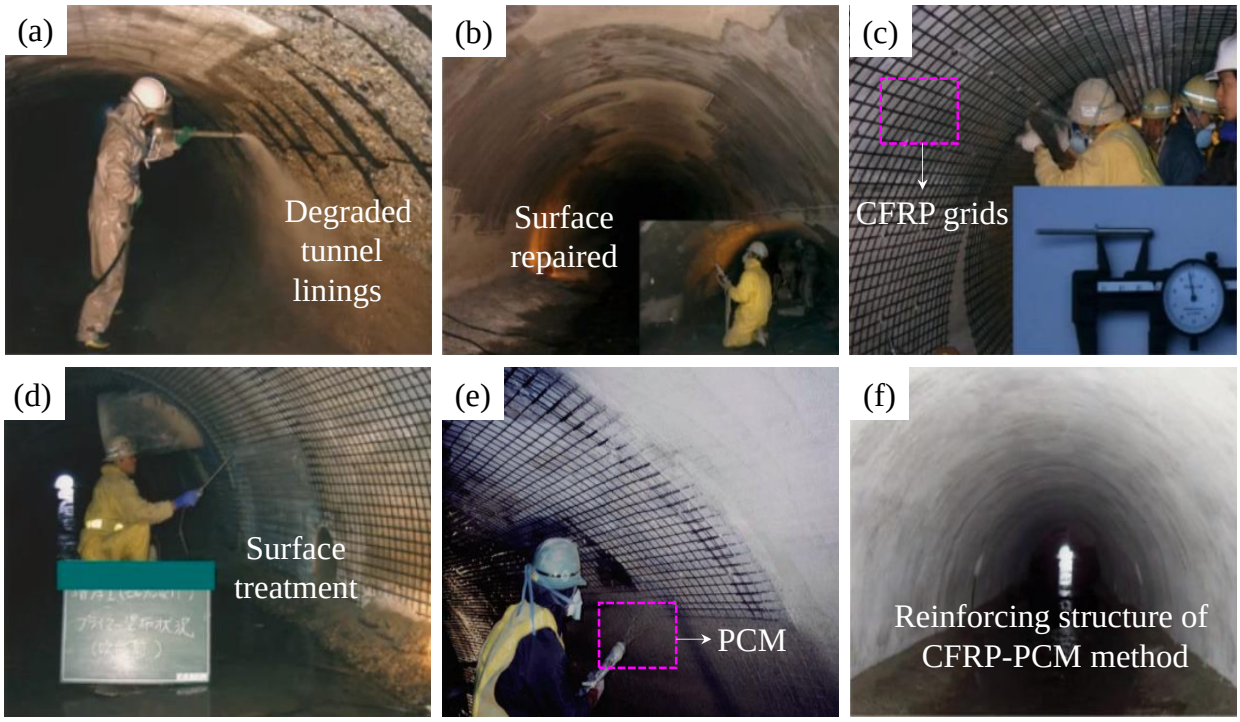

Fig. 1 Construction processes of the CFRP-PCM method on degraded tunnel linings (FRP Grid Method Association of Japan)

fix the CFRP grids to the lining concrete surface with rivets. Next, re-repair the lining surface to ensure smoothness. Finally, spray the PCM shotcrete onto the CFRP grids to form a complete reinforcing structure. Concerning the reinforcing effect of CFRP-PCM method, Yue *et al.* (2016) indicated that the bending and shear strengthening effect of RC members can be effectively improved with this method. Jiang *et al*. (2017) conducted laboratory direct shear tests and bending tests to investigate the bonding behavior between the PCM and the concrete reinforced by the CFRP grids, and three grades of CFRP grids (CR4, CR6, and CR8) were considered. Guo *et al*. (2018) proposed a new evaluation method for the shear capacity of RC beams reinforced by the CFRP-PCM method, and the effect of the arrangement of the CFRP grids was investigated.

Note that, extensive investigations have been conducted to explore the strengthening effect of CFRP materials on the concrete beam (straight structure), whereas information on the reinforcing behavior of the CFRP-PCM method on tunnel linings (arch structure) is rather limited, and its application should be further discussed. In addition, the unfavorable condition of the cavity behind the lining is widespread in operating tunnels. Unfortunately, investigations about the effect of the cavity on the strengthening behavior of the lining are much scarce. Therefore, this study aims to explore the reinforcing behavior of the CFRP-PCM method on degraded tunnel lining with a cavity. This study is expected to improve the understanding of the treatment of tunnel lining diseases.

2. Model establishment

An unfavorable condition, that is, there are cavities exist between the lining and the rock mass usually occur in mountain tunnels, resulting in insufficient lining thickness (Fraldi and Guarracino 2009, Fu *et al.* 2019, Hu *et al.* 2020). To explore the effect of the cavity on the tunnel lining, the numerical model established in this paper can be presented in Fig. 2. Note that the arc range of the cavity is 90° relative to the tunnel center point. Besides, it should be indicated that the polyester polyurethane was applied as the back-filling material. With respect to the size of the numerical model, the excavation diameter of the tunnel is D (10 m), while the horizontal distance from the wall to the model boundary is set as 2D to eliminate the boundary effects. Additionally, the lining thickness is 45 cm, which is reduced to 15 cm due to the existence of the cavity. Regarding the mesh quality, the rock mass and the lining concrete were modeled with solid elements. Specifically, the model was composed of 1978 elements and 4116 nodes. Concerning the boundary conditions, the left and right boundaries are rollers, while the bottom boundary is constrained completely. For the upper boundary, the loosening pressure is exerted on the tunnel lining. It should be indicated that the loosening pressure is caused by the cavity behind the lining, inducing the weight of the loosed rock mass to act directly on the tunnel lining. Specifically, the value of the loosening pressure is equal to the weight of the loosed rock mass in the loosening height, which was set as 2D in this research. Regarding the constitutive equations, the Mohr-Coulomb criterion was applied to describe the mechanical behavior of tunnel linings, CFRP grids, and PCM. In addition, the ground class of CII, DI, and DII were considered in this paper. The parameters of the ground, tunnel lining, and back-filling materials can be displayed in Table 1 (Jiang *et al.* 2017). It

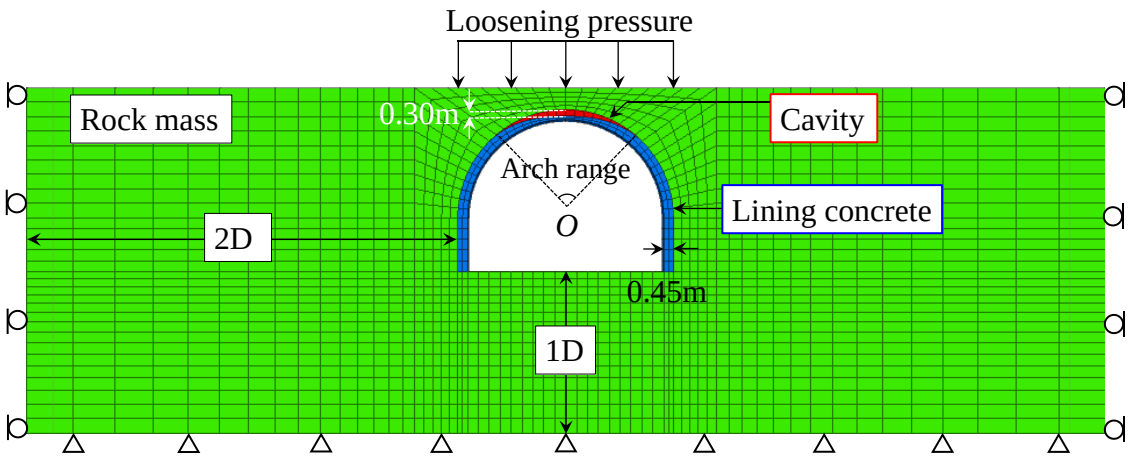

Fig. 2 Schematic diagram of the numerical model

Table 1 Parameters of ground, lining, and back-filling materials (Jiang *et al.* 2017)

Properties	Ground class			Lining	Back-filling materials
	CII	DI	DII		
γ (kN/m^3)	22.6	21.6	20.6	24	9.8
E (MPa)	980	490	147	24500	12.0
v	0.3	0.35	0.35	0.20	0.13
c (MPa)	0.98	0.49	0.196	6.99	0.50
φ (deg)	40.0	35.0	30.0	40.0	10.0
σ_t (MPa)	0.42	0.19	0.06	3.00	0.20

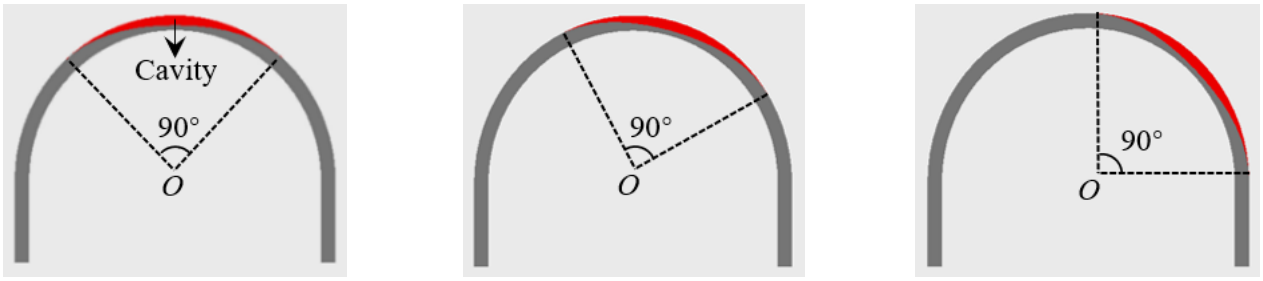

(a) Crown (b) Between crown and shoulder (c) Shoulder

Fig. 3 Position of the cavity between the lining and rock mass

should be noted that field investigations indicated that multiple cavities generally appear behind the tunnel lining concrete (Lalagüe *et al.* 2016, Ye and Ye 2019). Therefore, it is necessary to determine where the cavity will have a greater impact on the tunnel. In this paper, three positions of the cavity were considered, respectively crown, shoulder as well as the position between crown and shoulder, as shown in Fig.3.

3. Damage status of tunnel linings

3.1 Damage zone and deformation characteristics

In this section, the lining deterioration is set as 0% to determine the location where the damage is more serious. Fig. 4 presents the distribution of the lining damage zone with different cavity locations. Regarding the ground class of CII and DI, tensile damage always occurs in a small area near the cavity. Whereas for the ground class of DII, no matter where the cavity is, there will be a significant degree of tensile and shear damage. It should be indicated that the location of the shear damage generally occurs near the cavity. Note that when the cavity is at the shoulder, the lining generates a larger damage zone than the cavity is on the crown or between the crown and the shoulder. To quantitatively evaluate the lining damage behavior, the lining damage zone with different cavity positions is presented in Fig. 5. It can be observed that the ground class of DII is much easier to occur in a larger damage zone than that of CII and DI. Meanwhile, the damage elements in the shoulder are generally larger than that of elsewhere, indicating that the lining is more prone to generate the damage zone when the cavity is at the shoulder.

Fig. 6 presents the deformation characteristic and failure mechanism of linings with different cavity positions.

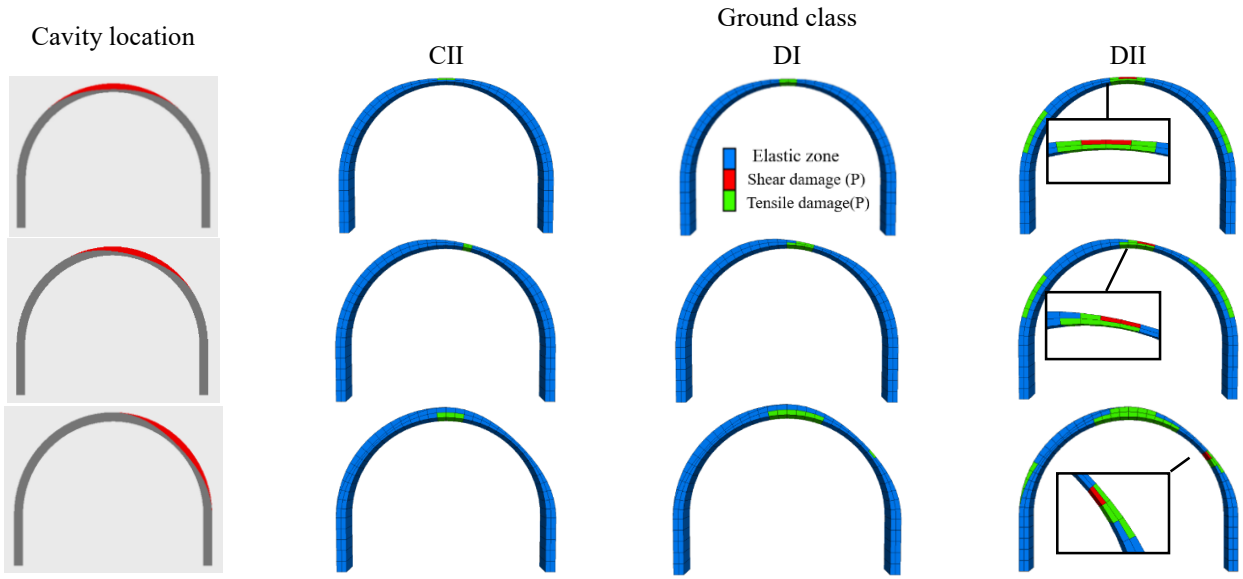

Fig. 4 Distribution of lining damage zone with different cavity locations

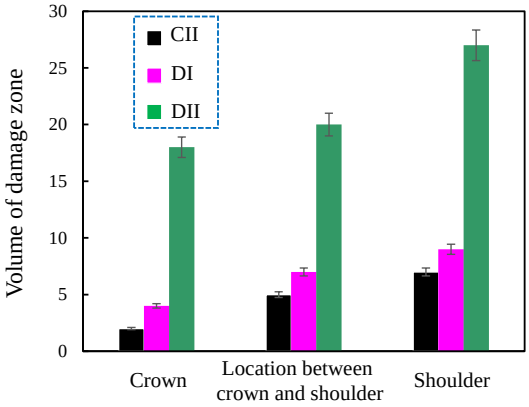

Fig. 5 Distribution of the damage zone of linings with a cavity located at different positions

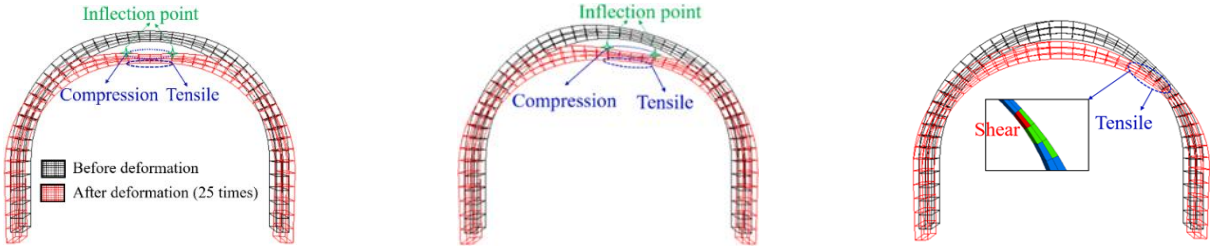

(a) Crown (b) Between crown and shoulder (c) Shoulder

Fig. 6 Deformation characteristics and failure mechanism of the lining with a cavity at different positions

According to Fig. 6, the deformation of the tunnel lining induced by the loosening pressure occurs significantly. Regarding a cavity located at the crown, the vertical deformation occurs symmetrically in the lining, resulting in crushing of the ground (compression failure due to bending compression), it is also noted that there are two inflection points in the linings after the lining deformation. Concerning a cavity located between the crown and the shoulder, the failure pattern is also induced by bending compression in the inner of the lining, and there are also two inflection points after deformation. Whereas for the shoulders, the vertical deformation is less than that of the above cases. In addition, the compression and tensile status in the lining are not changed, and there is no inflection point. Therefore, the failure pattern of the lining with a cavity at the shoulder is not caused by the compression and bending effect, combined with the distribution characteristics of the damage zone, it can be observed that the failure mechanism is caused by tensile and shear effect.

3.2 Shear stress in tunnel linings

Fig. 7 presents the shear stress of the lining at different

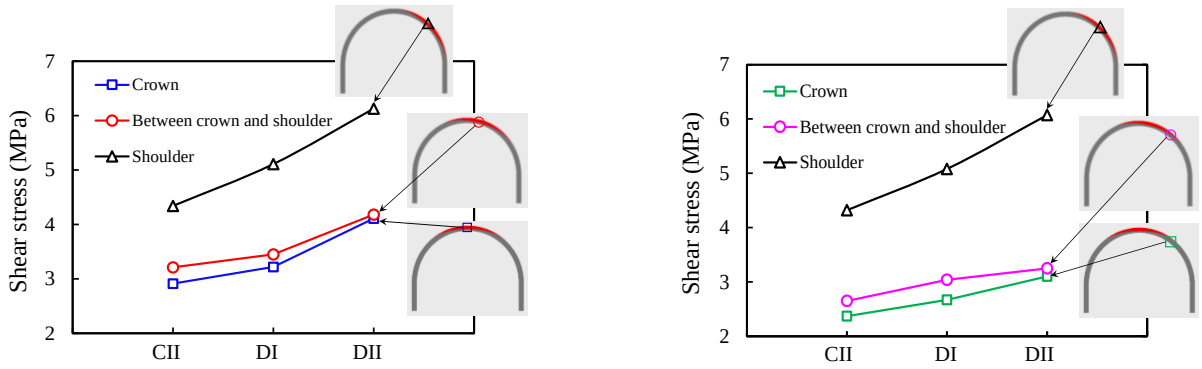

(a) Part in the thin lining (b) Shoulder in the lining

Fig. 7 Shear stress of the lining at different positions

Table 2 Parameters of the lining with different lining deterioration degrees

Deterioration degree (%)	E (MPa)	σ_c (MPa)	c (MPa)	φ(deg)	σ_t (MPa)
0	24,500	30.0	6.99	40.0	3.0
20	19,600	24.0	5.59		2.4
30	17,150	21.0	4.89		2.1
40	14,700	18.0	4.19		1.8
50	12,250	15.0	3.50		1.5
80	4,900	6.0	1.40		0.6

Table 3 Parameters of the CFRP grids and PCM materials (Jiang *et al.* 2017)

Reinforcing materials		E (MPa)	σ_t (MPa)	c_s (MPs)	φ_s (deg)	k_s (MPa/mm)
CFRP grids	CR4	100000	1400	2217	17.7	5.298
	CR6					6.394
	CR8					13.369
PCM		26000	4.60			—

positions under the loosening pressure. As shown in Fig. 7(a), when the cavity is at the shoulder, the shear stress of the lining is significantly larger than that of elsewhere. Specifically, when the grade of ground class is DII, the maximum shear stress is 6.2 MPa when the cavity is at the shoulder, whereas 3.75 MPa for the crown. In addition, the shear stress gradually increases as the grade of the ground class decreases. As can be seen from Fig. 7(b), the shear stress shows a negative correlation with the grade of the ground class. Note that the maximum shear stress when the cavity is at the shoulder is about 1.5 times that of other models, and so the shear stress in the shoulder with a cavity is larger than that of elsewhere. In other words, it can be regarded that the damage is most remarkable when the cavity is at the shoulder. Therefore, in next section, theoretical considerations are given regarding the selection of reinforcing methods for the cavity location at the shoulder. The ground class was determined as DI and DII. Besides, the deterioration degrees of tunnel lining can be summarized in Tables 2. In this research, three grades of CFRP grids were applied to reinforce the degraded tunnel linings with a cavity disease, and the corresponding parameters can be listed in Table 3 (Jiang *et al.* 2017).

4. Evaluation of the reinforcing behavior

4.1 Distribution of damage zone

In this section, the cavity at the shoulder was determined to investigate the reinforcing effect of the CFRP-PCM method on degraded tunnel linings, the region reinforced by the CFRP-PCM method covered an arc length of 90° and 180°on the upper wall of the tunnel can be presented in Fig. 8. When the degree of lining deterioration is larger (i.e., 80%), the distribution of the damage zone can be shown in Fig. 9. As observed in Fig. 9(a) (ground class of DI), when the degraded tunnel lining is not reinforced with the CFRP-PCM method, the crown would generate both tensile damage and shear damage. Meanwhile, a large range of shear damage occur at shoulders. In the cases of reinforcement covered an arc range of 90°, note that the reinforcing effect is similar with different grades of CFRP grids (CR4, CR6, and CR8). Specifically, the shear damage at the left shoulder and the crown is eliminated, meanwhile, the zone of tensile damage is also significantly reduced. When the reinforcement of the CFRP-PCM method covered an arc range of 180°, it is observed that the damage in the crown and the left shoulder is completely suppressed. Regarding the right shoulder of the lining, the damage zone also decreases significantly. As illustrated in Fig.9b (ground class of DII), when no reinforcing treatment was performed, a large amount of shear damage occurs at shoulders, and a large range of tensile damage as well as shear-tensile damage generates at the crown. The lining suffers large-scale damage at this time, which can be regarded as the dangerous situation. In the cases of reinforcement covered an arc range of 90°, the failure at the right shoulder is changed from a large amount of shear damage to a small amount of tensile damage. When the reinforcement of the CFRP-PCM method covered an arc range of 180°, the tensile and shear damage at the crown can be suppressed, and the shear damage at the shoulder also changes to a small amount of tensile damage. In addition, the reinforcing effect of CR6 and CR8 is more apparent than that of CR4.

(a) 90° (b) 180°

Fig. 8 Arc range of the CFRP-PCM method

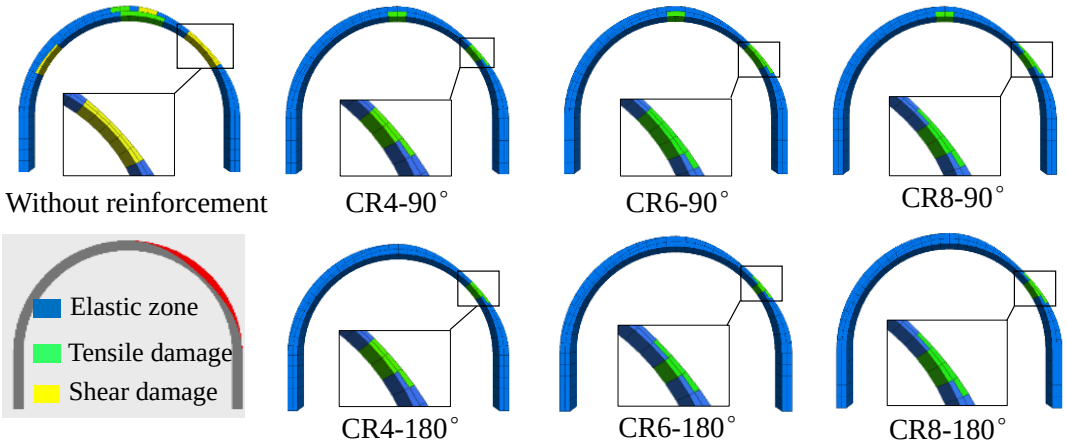

(a) Ground class of DI

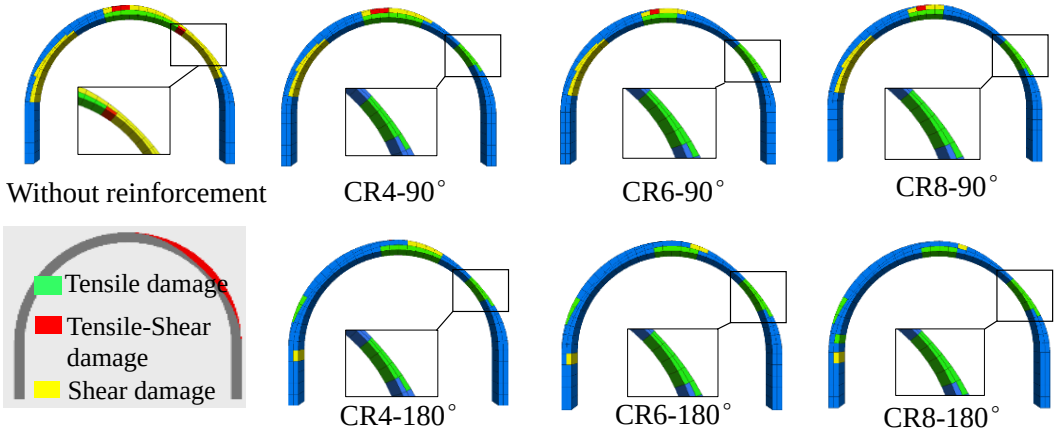

(b) Ground class of DII

Fig. 9 Distribution of damage zone with different reinforcing schemes under the lining deterioration degree of 80%

To quantitatively evaluate the reinforcing effect of the CFRP-PCM method on degraded tunnel linings, the damage rate of lining under different deterioration degrees (i.e., 0%, 50%, and 80%) for the ground class of DI and DII was summarized in Fig. 10. It should be indicated that the damage rate of lining in this research is defined as the ratio of the volume of damaged elements to the volume of total elements. When the lining deterioration is 0%, 50%, and 80%, the lining damage rate can be presented in Fig.10(a)-10(c). Note that the application of the CFRP-PCM method could significantly reduce the damage rate of lining except for the case of CR4-DI-90°. Here, CR4 represents the grade of the CFRP grids, DI stands for the ground class, 90° represents the arc range of the reinforcement. In addition, it is obvious that when the arc range of CFRP grids is 180°, the damage rate of lining is less than that of 90°. As can be seen from Fig.10(b) and 10(c), as the grade of CFRP grids increases (i.e., from CR4 to CR8), the damage rate of lining decreases significantly, indicating the reinforcing effect becomes better. Specifically, the damage rate of the lining decreased by 45.9% from no anchoring measures to CR4-90°, while from CR4 to CR8, it only decreased by 28.3%. By comparing Fig.10(a)-10(c), note that the higher the deterioration degree of tunnel linings, the more significant the CFRP-PCM method on restraining the damage rate.

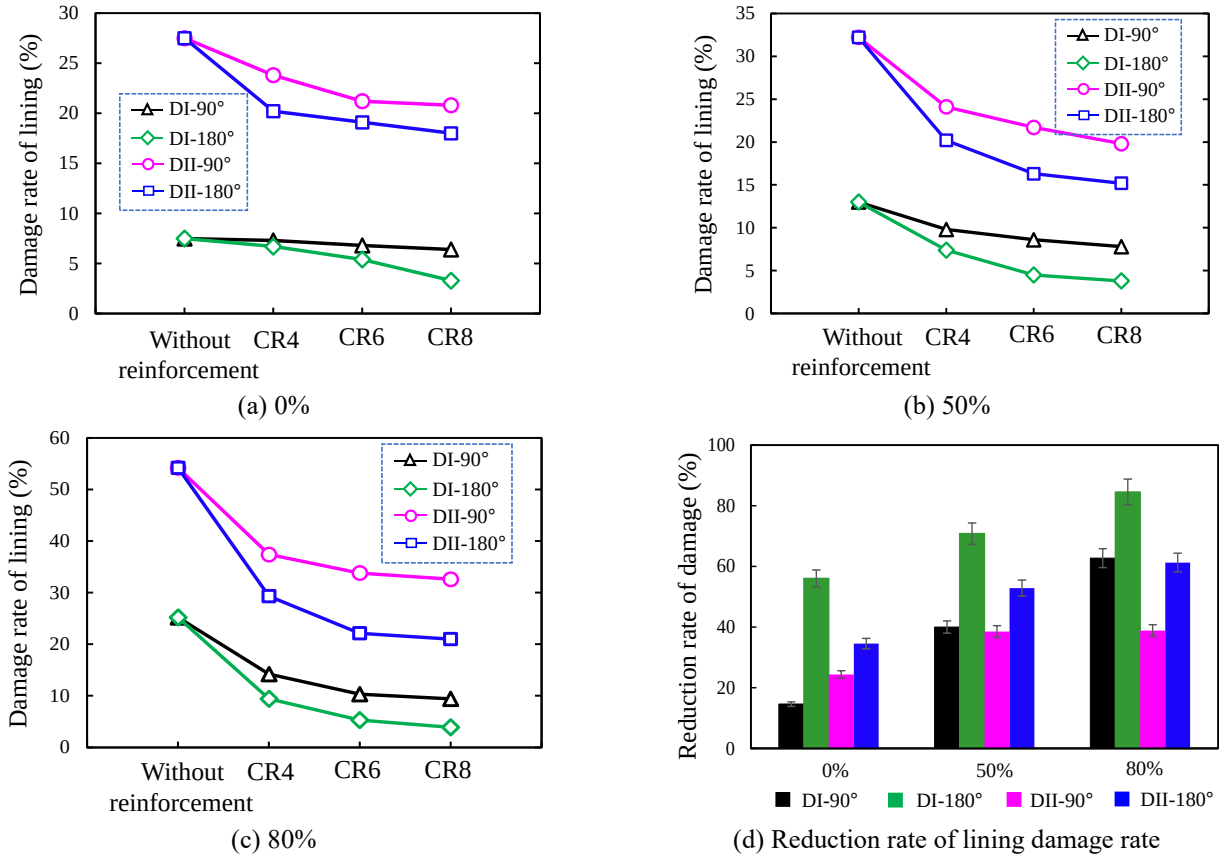

Fig. 10 Damage rate of lining with different deterioration degrees

Fig.10(d) shows the reduction rate of the lining damage rate from no reinforcement measure to the reinforced by the CFRP(CR8)-PCM method. Concerning the ground class of DI, when the lining deterioration degree is 0%, the reduction rate of damage rate is 18.4% for the arc range of 90°, while 57.6% for the 180°. Regarding the ground class of DII, when the lining deterioration degree is 50% and 80%, the reinforcing effect of the CFRP-PCM method covered an arc range of 180° can be better to control the lining damage rate than the 90° significantly. Analogously, as the comparison between Fig.10(a)-10(d), the reinforcing effect of the CFRP-PCM method is also significantly affected by the grade of the ground class. Taking the lining with the deterioration of 80% as an example (Fig. 10(c)), when the degraded lining changes from no reinforcing treatment to the reinforcement of the CFRP(CR8)-PCM method, the average reduction value of the damage rate is 27.4% for the ground class of DII, while 18.55% for the ground class of DI. Therefore, the lower the grade of the ground class, the larger the reduction in the lining damage rate.

4.2 Reduction rate of shear stress

Fig. 11 presents the distribution of the maximum shear stress with a lining deterioration degree of 80%. As observed from Fig. 11(a) (ground class of DI), when there is no reinforcement, the maximum shear stress is 2.97 MPa, which is located at the right shoulder. When the CFRP-PCM method was applied to reinforce the degraded linings, represents the maximum shear stress decreases obviously. Specifically, 0.67 MPa for CR4, 0.56 MPa for CR6, and 0.52 MPa for CR8 when the arc range of the reinforcement is 90°; 0.61 MPa for CR4, 0.51 MPa for CR6, and 0.49MPa for CR8 when the reinforcing range is 180°. Note that the maximum shear stress is smaller when the anchoring range is 180° compared to the arc range of 90°. Analogously, when the ground class is DII, the distribution of maximum shear stress can be presented in Fig. 11(b). It can be observed that the maximum shear stress can be significantly reduced with the application of the CFRP-PCM method. In addition, the maximum shear stress of the lining without the reinforcement is all distributed near the cavity, and when the CFRP-PCM method was utilized for reinforcement with an arc range of 90°, the maximum shear stress is located at the symmetrical position of the cavity, whereas for the reinforcement with an arc range of 180°, the maximum shear stress is located at the left wall of the tunnel lining.

In this section, the reduction rate of the maximum shear stress with the reinforcement of the CFRP-PCM method was investigated. When the lining is without a deterioration, the reduction rate of the maximum shear stress can be presented in Fig.12(a). With the increment of the grade of CFRP grids, the reduction rate increases significantly. Note that when the arc range of CFRP grids is 90° for the ground class of DI, the reduction rate is 52.7%, 56.8%, and 60.7% for CR4, CR6, and CR8, showing an approximately linear manner. Analogously, when the arc range of CFRP grids is 90° for the ground class of DII, the reduction rate also presents an approximately linear relation as the grade of

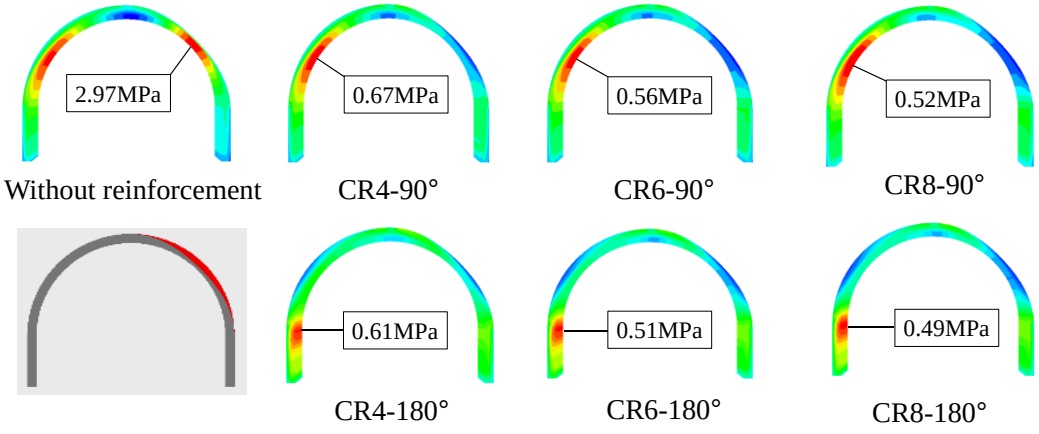

(a) Ground class of DI

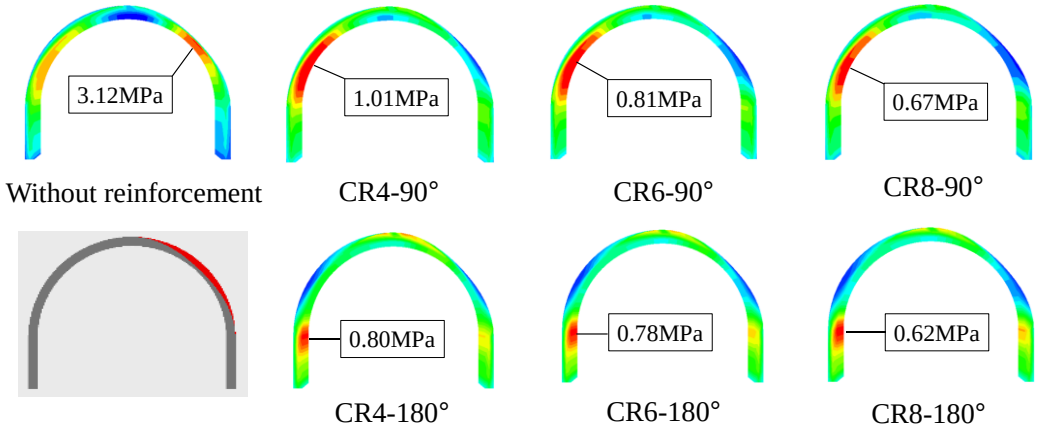

(b) Ground class of DII

Fig. 11 Distribution of maximum shear stress with a lining deterioration degree of 80%

CFRP grids changes from CR4 to CR8. However, when the arc range of CFRP grids is 180° for the ground class of DI, the reduction rate is 60.5%, 66.4%, and 68.6% for CR4, CR6, and CR8, showing a decreases trend. In addition, note that the reduction rate of the maximum shear stress with the arc range of 180° is always larger than that of 90°. Fig. 12(b) shows curves of the reduction rate of the maximum shear stress with the reinforcement of the CFRP-PCM method when the lining deterioration degree is 50%. When the arc range of CFRP grids is 90° for the ground class of DI, the reduction rate is 60.8%, 72.5%, and 77.8% for CR4, CR6, and CR8, showing an approximately linear manner, while for the arc range of 180°, the reduction rate presents a decreasing trend as the grade of CFRP grids changes from CR4 to CR8. When the ground class is DII, the reduction rate increases as the grade of CFRP grids increases. The reduction rate of the maximum shear stress evolves with the grade of CFRP grids under the lining deterioration degree of 80% can be revealed in Fig. 12(c), when the CR4 and CR6 were applied in DI, the reduction rate of the shear stress with the arc range of 90° is greater than that of 180°, while for DII, the reduction rate of the maximum shear stress with the CR8 under the arc range of 180° is larger than that of 90°. Therefore, it can be observed that the reduction rate of the maximum shear stress with the reinforcement of the CFRP-PCM method is not only affected by the ground class but also the lining deterioration degree.

4.3 M-N interaction curve for degraded tunnel linings

The M-N interaction curves have been proposed to investigate the limit state design method of the structure. In this paper, the M-N theoretical interaction curves with the lining deterioration of 0%, 20%, 30%, 40%, 50%, and 80% can be presented in Fig. 13. It should be indicated that the theoretical values of M-N interaction curves of tunnel linings with different lining deterioration degrees can be obtained according to the Japan Iron and Steel Federation Steel Fiber Reinforced Concrete Revision Committee (2002). The numerical inner force of the lining was subsequently calculated and compared with the corresponding M-N theoretical curves. If the coordinates of the axial force and bending moment are inside the interaction curve, the lining is in a safe state.

Fig. 13(a)-13(e) present the comparison between the numerical inner force values and the theoretical values at the shoulder and crown when the lining deterioration is 0%, 20%, 30%, 40%, and 50%, respectively. It is observed that the coordinate of the (M, N) is all situated at the inner side

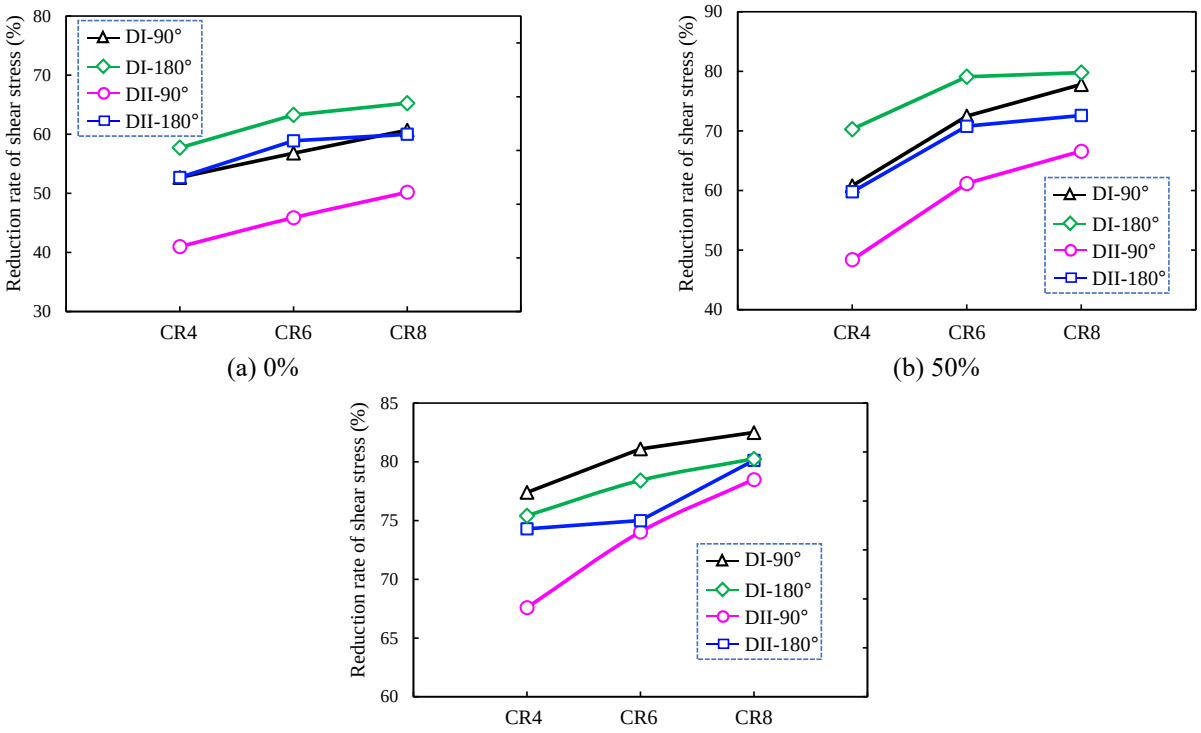

Fig. 12 Reduction rate of the maximum shear stress with different lining deterioration degrees

of the corresponding M-N interaction curves, revealing that the lining is in a safe state. However, when the lining deterioration is 80% (Fig.13(f)), the below four reinforcing designs of "CR6-2D-120°-Crown", "CR8-2D-120°-Crown", "CR4-2D-180°-Shoulder", and "CR6-2D-90°-Shoulder" are distributed outside of the corresponding M-N interaction curves for the ground class of DI. Whereas for the ground class of DII, the below six reinforcing designs of

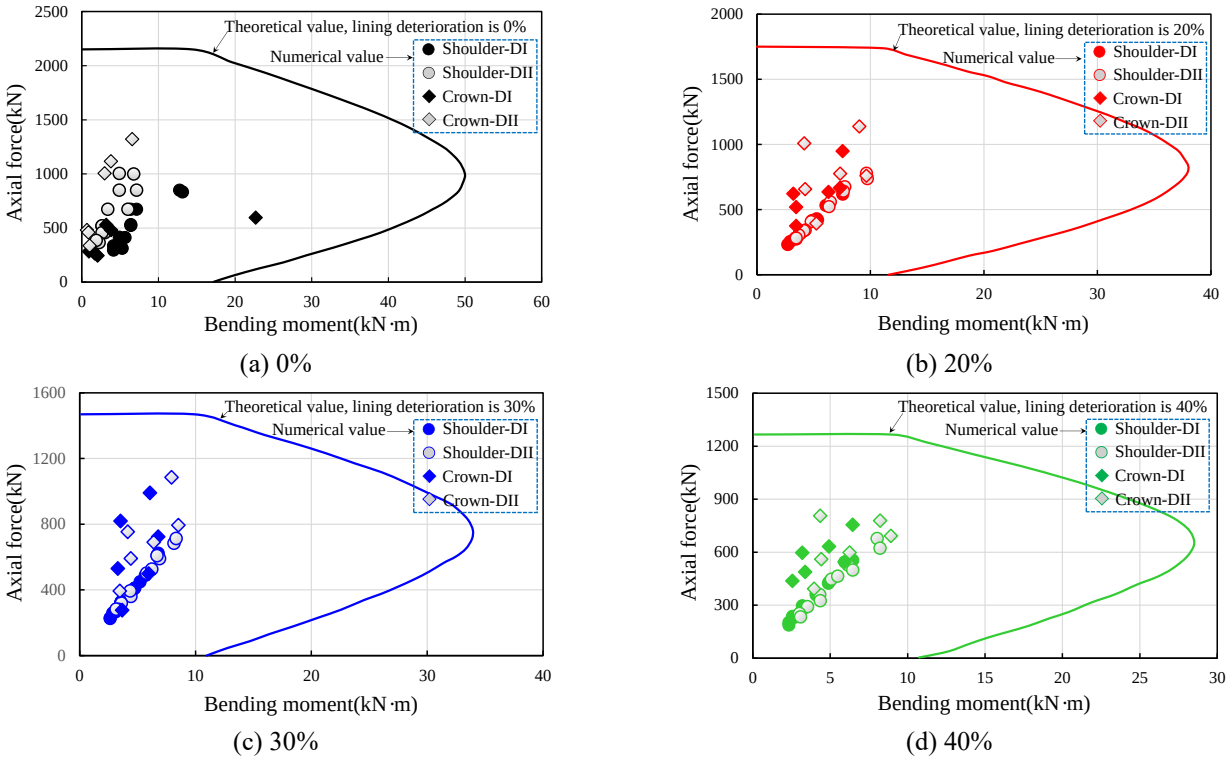

Fig. 13 M-N theoretical and numerical values with different lining deterioration degrees

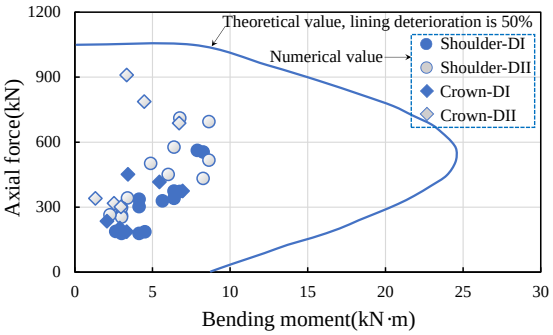

(e) 50%

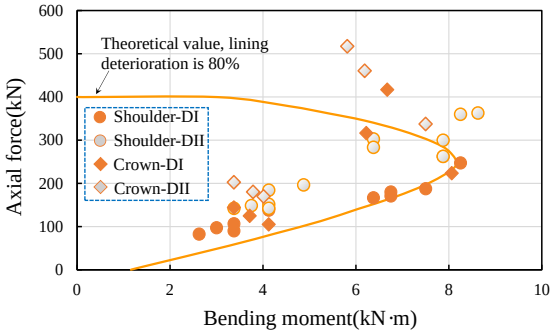

(f) 80%

Fig. 13 Continued

"CR4-2D-120°-Crown", "CR6-2D-120°-Crown", "CR8-2D-120°-Crown", "CR4-2D-90°-Shoulder", "CR4-2D-180°-Shoulder", "CR6-2D-90°-Shoulder" are distributed outside of the corresponding M-N interaction curves. Therefore, the above ten reinforcing designs should be avoided in the corresponding reinforcing engineering with the CFRP-PCM method.

5. Conclusions

This research investigated the CFRP-PCM method to reinforce the degraded tunnel linings. At first, the most unfavorable position for the cavity behind the lining was determined. Subsequently, the reinforcing effect of the CFRP-PCM method was quantitatively evaluated. Finally, the M-N interaction curves were applied to determine whether the reinforcing design is effective. The main conclusions can be drawn as follows:

- The damage behavior of tunnel linings under the loosening pressure is closely related to not only the ground class but also the location of the cavity. The lower the grade of ground class, the larger the damage zone; When the cavity is located at the shoulder, the damage rate and maximum shear stress of the lining are larger than those at other positions, which is determined as the most unfavorable position.
- The failure mechanism of the lining under the loosening pressure is significantly affected by the location of the cavity. When the cavity is at the crown and the location between the crown and the shoulder, the failure modes are dominated by the bending compression effect. However, when the cavity is at the shoulder, the mixed tensile-shear effect dominates the failure of the lining.
- The reinforcing effect of the CFRP-PCM method is affected by the arch range of the CFRP grids, the grade of CFRP grids, the degree of ground class, and the deterioration rate of the lining. Specifically, the larger the arc range of the CFRP grids, the smaller the lining damage rate. In general, the higher the grade of the CFRP grids, the larger the reduction rate of shear stress; the higher the deterioration degree of lining and the lower the degree of ground class, the better the reinforcing effect under the same CFRP grids. However, as the grade of the CFRP grid increases, the optimization effect is no longer obvious.
- The M-N interaction curves can be well applied to estimate the reinforcing behavior of the CFRP-PCM method. Note that when the lining deterioration is 80%, the M-N values of the ten reinforcing designs of the CFRP-PCM method are distributed outside the corresponding M-N theoretical interaction curves, which indicated that although the tunnel lining can be reinforced to a certain extent with the CFRP-PCM method, some reinforcement schemes still cannot meet the safety requirements (four cases for the ground class of DI and six cases for ground class of DII in this research), and these reinforcing schemes should be avoided in the corresponding engineering.

Acknowledgments

The authors gratefully acknowledge support of Civil Engineering Department, Technical Division, Konoike Construction Japan for sharing experience on tunnel construction and the experience from the FRP Grid Method Association of Japan.

References

Aalianvari, A. (2017), "Combination of engineering geological data and numerical modeling results to classify the tunnel route based on the groundwater seepage", *Geomech. Eng.*, **13**(4), 671-683. http://doi.org/10.12989/gae.2017.13.4.671.

Bansal, P.P. and Sidhu, R. (2017), "Mechanical and durability properties of fluoropolymer modified cement mortar", *Struct. Eng. Mech.*, **63**(3), 317-327. http://doi.org/10.12989/sem.2017.63.3.317.

Benzaama, A., Mokhtari, M., Benzaama, H., Gouasmi, S. and Tamine, T. (2018), "Using XFEM technique to predict the damage of unidirectional CFRP composite notched under tensile load", *Adv. Aircraft Spacecr. Sci.*, **5**(1), 129-139. https://doi.org/10.12989/aas.2018.5.1.129.

Fang, H., Xu, X., Liu, W.Q., Qi, Y.J., Bai, Y., Zhang, B. and Hui, D. (2016), "Flexural behavior of composite concrete slabs reinforced by FRP grid facesheets", *Compos. Part B Eng.*, **92**, 46-62. https://doi.org/10.1016/j.compositesb.2016.02.029.

Feiteira, J. and Ribeiro, M.S. (2013), "Polymer action on alkali-silica reaction in cement mortar", *Cement Concrete Res.*, **44**, 97-105. https://doi.org/10.1016/j.cemconres.2012.09.008.

Fraldi, M. and Guarracino, F. (2009), "Limit analysis of collapse

mechanisms in cavities and tunnels according to the Hoek-Brown failure criterion", *Int. J. Rock Mech. Min. Sci.*, **46**(4), 665-673. https://doi.org/10.1016/j.ijrmms.2008.09.014.

FRP Grid Method Association of Japan (n.d), Design and construction manual of the Repair & reinforcement method for RC structures by FRP grid [O/L], http://www.frp-grid.com/01.html.

Fu, J.Y., Xie, J.W., Wang, S.Y., Yang, J.S., Yang, F. and Pu, H. (2019), "Cracking performance of an operational tunnel lining due to local construction defects", *Int. J. Geomech.*, **19**(4), 04019019. https://doi.org/10.1061/(ASCE)GM.1943-5622.0001371.

Gaurav, A. and Signh, K.K. (2018), "Fatigue behavior of FRP composites and CNT-Embedded FRP composites: A review", *Polym. Composite*, **39**(6), 1785-1808. https://doi.org/10.1002/pc.24177.

Ghasemi, S.H. and Nowak, A.S. (2018), "Reliability analysis of circular tunnel with consideration of the strength limit state", *Geomech. Eng.*, **15**(3), 879-888. http://doi.org/10.12989/gae.2018.15.3.879.

Guler, S., Oker B. and Akbulut Z.F. (2021), "Workability, strength and toughness properties of different types of fiber-reinforced wet-mix shotcrete", *Structure*, **31**, 781-791. https://doi.org/10.1016/j.istruc.2021.02.031.

Guler, S. and Yavuz, D. (2019), "Post-cracking behavior of hybrid fiber-reinforced concrete-filled steel tube beams", *Constr. Build. Mater.*, **205**, 285-305. https://doi.org/10.1016/j.conbuildmat.2019.01.192.

Guler, S., Yavuz, D. and Aydin M. (2019), "Hybrid fiber reinforced concrete-filled square stub columns under axial compression", *Eng. Struct.*, **198**, 109504. https://doi.org/10.1016/j.engstruct.2019.109504.

Guler, S., Yavuz, D., Korkut, F. and Ashraf, A. (2018), "Strength prediction models for steel, synthetic, and hybrid fiber reinforced concretes", *Struct. Concrete*, **20**(1), 428-445. https://doi.org/10.1002/suco.201800088.

Guo, R., Pan, Y., Cai, L.H. and Hino, S. (2018), "Study on design formula of shear capacity of RC beams reinforced by CFRP grid with PCM shotcrete method", *Eng. Struct.*, **166**, 427-440. https://doi.org/10.1016/j.engstruct.2018.03.095.

Hu, J., Li, S.C., Liu, H.L., Li, L.P., Shi, S.S. and Qin, C.S. (2020), "New modified model for estimating the peak shear strength of rock mass containing nonconsecutive joint based on a simulated experiment", *Int. J. Geomech.*, **20**(7), 1-10. https://doi.org/10.1061/(ASCE)GM.1943-5622.0001732.

Japan Iron and Steel Federation Steel Fiber Reinforced Concrete Revision Committee (2002), *Steel Fiber Reinforced Concrete Design and Construction Manual*, GIHODO SHUPPAN Co., Ltd, Tokyo, Japan.

Jeffrey, J.B., Lawrence, C.B. and Michael, G.O. (2016), "Punching shear failure in double-layer pultruded FRP grid reinforced concrete bridge decks", *Adv. Struct. Eng.,* **15**(4), 601-613. https://doi.org/10.1260/1369-4332.15.4.601.

Jeng, F., Lin, M.L. and Yuan, S.C. (2002), "Performance of toughness indices for steel fiber reinforced shotcrete", *Tunn. Undergr. Sp. Tech.*, **17**(1), 69-82. https://doi.org/10.1016/S0886-7798(01)00065-7.

Jiang, Y.J., Wang, X.S., Li, B., Higashi, Y., Taniguchi, K. and Ishid, K. (2017) "Estimation of reinforcing effects of FRP-PCM method on degraded tunnel linings", *Soils Found.*, **57**, 327-340. https://doi.org/10.1016/j.sandf.2017.05.002.

Joong, K.J. Woo, S.K. Gyu, Y.K. and Chan, K.J. (2016), "Polyamide fiber reinforced shotcrete for tunnel application", *Materials*, **9**(3), 163. https://doi.org/10.3390/ma9030163.

Kishi, N., Zhang, G. and Mikami, H. (2005), "Numerical cracking and debonding analysis of RC beams reinforced with FRP sheet", *J. Compos. Constr.*, **9**(6), 507-514. https://doi.org/10.1061/(asce)1090-0268(2005)9:6(507).

Lalagüe, A., Lebens, M.A., Hoff, I. and Grøv, E. (2016), "Detection of rockfall on a tunnel concrete lining with ground-penetrating radar (GPR)", *Rock Mech. Rock Eng.*, **49**(7), 2811-2823. https://doi.org/10.1007/s00603-016-0943-y.

Lee, J.K. and Lee, J.H. (2002), "Nondestructive evaluation on damage of carbon fiber sheet reinforced concrete", *Compos. Struct.*, **58** (1), 139-147. https://doi.org/10.1016/S0263-8223(02)00029-6.

Li, Z.X., Li, C.H., Shi Y.D. and Zhou X.J. (2017), "Experimental investigation on mechanical properties of hybrid fibre reinforced concrete", *Constr. Build. Mater.*, **157**, 930-942. https://doi.org/10.1016/j.conbuildmat.2017.09.098.

Maalej, M. and Leong, K.S. (2005), "Effect of beam size and FRP thickness on interfacial shear stress concentration and failure mode of FRP-strengthened beams", *Compos. Sci. Technol.*, **65**(7), 1148-1158. https://doi.org/10.1016/j.compscitech.2004.11.010.

Makeev, A., Ghaffari, S. and Seon, G. (2019), "Improving compressive strength of high modulus carbon-fiber reinforced polymeric composites through fiber hybridization", *Int. J. Eng. Sci.*, **142**, 145-157. https://doi.org/10.1016/j.ijengsci.2019.06.004.

Mofidi, A. and Chaallal, O. (2014), "Tests and design provisions for reinforced-concrete beams strengthened in shear using FRP sheets and strips", *Int. J. Concr. Struct. Mater.*, **8**(2), 117-128. https://doi.org/10.1007/s40069-013-0060-1.

Nishi, Y., Tsuchikura, N., Nanba, S., Yamamoto, T. and Faudree, M.C. (2012), "Charpy impact of sandwich structural composites (CFRP/PC/CFRP) of polycarbonate (PC) cores covered with carbon fiber cross textile reinforced epoxy polymer (CFRP) thin sheets as a function of temperature", *Mater. Trans.*, **53**(7), 1288-1294. https://doi.org/10.2320/matertrans.M2011357.

Rabia, B., Hassaine, T. and Abderezak. (2019), "Effect of distribution shape of the porosity on the interfacial stresses of the FGM beam strengthened with FRP plate", *Earthq. Struct.*, **16**(5), 601-609. http://doi.org/10.12989/eas.2019.16.5.601.

Rajak, D.K., Pagar, D.D., Menezes, P.L. and Linul, E. (2019), "Fiber-reinforced polymer composites: Manufacturing, properties, and applications", *Polymers*, **11**, 1667. https://doi.org/10.3390/polym11101667.

Razavi, M.R. and Mustaffa, Z. (2018), "Rehabilitation of notched circular hollow sectional steel beam using CFRP patch", *Steel Compos. Struct.*, **26**(2), 151-161. http://doi.org/10.12989/scs.2018.26.2.151.

Schrefler, B.A., Codina, R. and Principe, F.P. (2011), "Thermal coupling of fluid flow and structural response of a tunnel induced by fire", *Int. J. Numer. Meth. Eng.*, **87**(1-5), 361-385. https://doi.org/10.1002/nme.3077.

Singh, S. and Patra, N.R. (2020), "Axial dynamic response of concrete-filled tapered fiber reinforced polymer piles in a transversely isotropic medium", *Comput. Geotech.*, **123**, 103557. https://doi.org/10.1016/j.compgeo.2020.103557.

Sukontasukkul, P., Pongsopha, P., Chindaprasirt, P. and Songpiriyakij, S. (2018), "Flexural performance and toughness of hybrid steel and polypropylene fibre reinforced geopolymer", *Constr. Build. Mater.*, **161**(2), 37-44. https://doi.org/10.1016/j.conbuildmat.2017.11.122.

Sumathi, A. and Arun, V.S. (2017), "Study on behavior of RCC beams with externally bonded FRP members in flexure", *Adv. Concr. Constr.*, **5**(6), 625-638. http://doi.org/10.12989/acc.2017.5.6.625.

Tonon, F. (2010), "Sequential excavation, NATM and ADECO: What they have in common and how they differ", *Tunn. Undergr. Sp. Tech.*, **25**(3), 245-265. https://doi.org/10.1016/j.tust.2009.12.004.

Ye, Z.J. and Ye, Y. (2019), "Comparison of detection effect of cavities behind shield tunnel segment using transient electromagnetic radar and ground penetration radar", *Geotech. Geol. Eng.*, **37**(5), 4391-4403. https://doi.org/10.1007/s10706-019-00916-y.

Yue, Q.R., Liu, Z.Q., Li, R. and Chen, X.B. (2016), "Experimental investigation into the development length of carbon-fiber-reinforced polymer grids in concrete", *Adv. Struct. Eng.*, **20**(6), 953-962. https://doi.org/10.1177/1369433216668360.

CC